# Cloud-CFFR: Coordinated Fractional Frequency Reuse in Cloud Radio Access Network (C-RAN)

# Abolfazl Hajisami and Dario Pompili

Dept. of Electrical and Computer Engineering, Rutgers University–New Brunswick, NJ, USA E-mails: {hajisamik, pompili}@cac.rutgers.edu

Abstract—Fractional Frequency Reuse (FFR) and Coordinated MultiPoint (CoMP) processing are two of the conventional methods to mitigate the Inter-Cell Interference (ICI) and to improve the average Signal-to-Interference-plus-Noise Ratio (SINR). However, FFR is associated with low system spectral efficiency and CoMP does not take any action to mitigate the inter-cluster interference. In the context of Cloud Radio Access Network (C-RAN) – a new centralized paradigm for broadband wireless access that addresses efficiently the fluctuation in capacity demand through real-time Virtual Base Station (VBS) cooperation in the Cloud - in this paper an innovative uplink solution, called Cloud-CFFR, is proposed to address the aforementioned problems. With respect to both FFR and CoMP, Cloud-CFFR decreases the complexity, delay, and ICI while increasing the system spectral efficiency. Since the system performance in celledge regions relies on the cooperation of different VBSs, there is no service interruption in handling handovers; moreover, in order to address the unanticipated change in capacity demand, Cloud-CFFR dynamically changes the sub-band boundaries based on the number of active users in the clusters. Simulation results confirm the validity of our analysis and show the benefits of this novel uplink solution.

Index Terms—Cloud Radio Access Network, Coordinated MultiPoint Processing, Fractional Frequency Reuse, Virtualization.

# I. INTRODUCTION

Motivation: Over the last few years, the proliferation of personal mobile computing devices like tablets and smartphones along with a plethora of data-intensive mobile applications has resulted in a tremendous increase in demand for high data-rate wireless communications. Current practice to enhance spectral efficiency and data rate is to increase the number of Base Stations (BSs) and go for smaller cells so to increase the band reuse factor. However, with small cells the Mobile Stations (MSs) experience a higher number of handovers and the Inter-Cell Interference (ICI) problem becomes more challenging which calls for interference management techniques.

Conventional Interference-management Techniques: Fractional Frequency Reuse (FFR) is an Inter-Cell Interference Coordination (ICIC) technique in OFDMA-based wireless network, which partitions the frequency band so that the interference received/created by MSs is reduced. There are two main types of FFR deployments presented in the literature, namely  $Strict\ FFR$  and  $Soft\ FFR$  [1]. Strict FFR, as shown in Fig. 1(a), is a modification of the traditional frequency reuse used extensively in multi-cell networks; neighboring cells are divided into clusters of M cells each, and the frequency band is partitioned into M+1 sub-bands.

To decrease the ICI, the cell-center MSs are allocated with a common sub-band while the rest of sub-bands are assigned to the cell-edge MSs based on a frequency reuse factor of 1/M. Although Strict FFR decreases the ICI, it results in poor overall frequency reuse. To alleviate this problem, Soft FFR uses the same cell-edge bandwidth partitioning strategy, but the cell-center MSs are allowed to use the sub-band frequencies allocated to the cell-edge MSs of the other cells. This strategy leads to a higher availability of resources (Fig. 1(b)); nevertheless, it generates more interference to both cell-center and cell-edge MSs than Strict FFR [1]. Last, but not least, partition sizes in FFR schemes are not adaptive to dynamic changes in capacity demand, which makes FFR not able to handle the unanticipated fluctuations in the number of users.

The Coordinated MultiPoint (CoMP) transmission and reception technique, which is based on cooperative Multiple Input Multiple Output (MIMO), is another method to mitigate the average interference and to increase the spectral efficiency at the cost of a higher receiver complexity [2]. In CoMP, a set of neighboring cells are divided into *clusters*; within each cluster, the BSs are connected with each other via a fixed Backhaul Processing Unit (BPU) and exchange Channel State Information (CSI) as well as MS signals to cancel the intra-cluster interference (Fig. 1(c)). However, CoMP is not able to mitigate the inter-cluster interference. Hence, the achieved system capacity - while improved - is still significantly far from the interference-free capacity upper bound, especially in environments with strong Co-Channel Interference (CCI). Furthermore, one of the main requisites of Long Term Evolution (LTE) systems is the very low level of latency: the additional processing required for multiplesite reception/transmission and CSI acquisition as well as the communication incurring among different BSs could add delay significantly and limits the cluster size (especially for massive MIMO). In addition to low-latency inter-BS communication, BS clocks need to be in phase in order to enable proper operation of CoMP, which requires a highly accurate phase or time-of-day synchronization. To overcome these challenges, the BSs should be connected together in a form of centralized Radio Access Network (RAN).

A New Cellular Network Paradigm: Cloud Radio Access Network (C-RAN) [3], [4] is a new architecture for wireless cellular networks that addresses the fluctuation in capacity demand efficiently while keeping the cost of delivering services

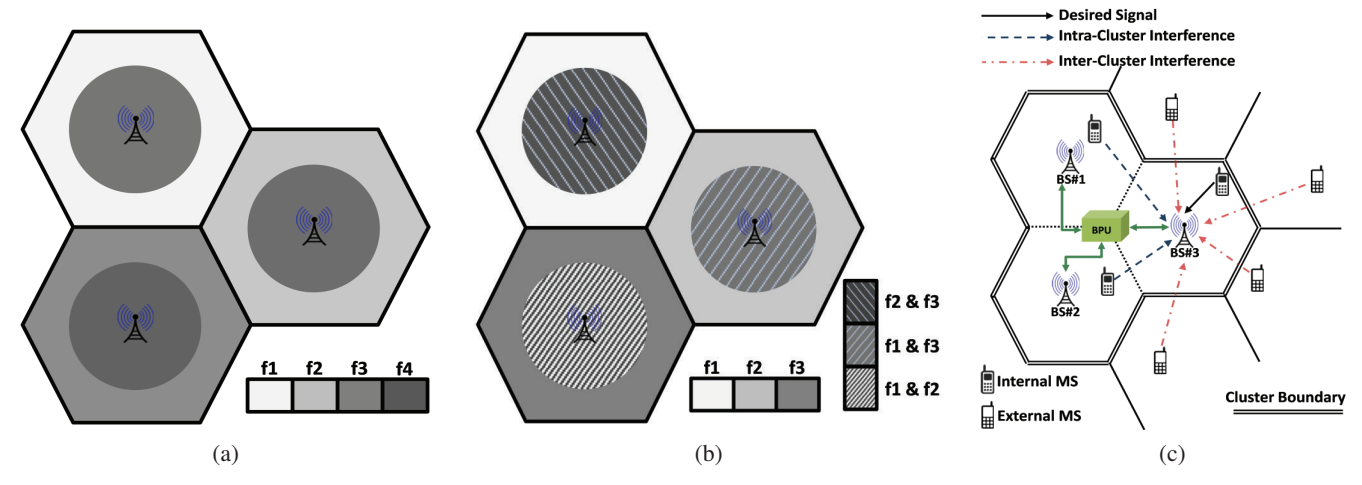


Fig. 1. (a) Strict-FFR and (b) Soft-FFR deployments with cell-edge reuse factor of 1/3; (c) Intra-cluster and inter-cluster interference in the uplink (we name the MS (BS) inside the cluster as *internal* MS (BS) and outside the cluster as *external* MS (BS)). In Coordinated MultiPoint (CoMP) processing BSs cooperate with each other and exchange data through Backhaul Processing Unit (BPU) in order to cancel the intra-cluster interference.

to the users low. It also provides a higher degree of cooperation and communication among BSs. C-RAN represents a cleanslate design and allows for dynamic reconfiguration of computing and spectrum resources. Characteristics of C-RAN are: i) centralized management of computing resources, ii) collaborative communications, and iii) real-time cloud computing on generic platforms. As shown in Fig. 2(a), C-RAN is composed of Remote Radio Heads (RRHs) distributed over a wide geographic region controlled by remote Virtual Base Stations (VBSs) housed in a centralized processing pools. VBSs and their corresponding RRHs are connected by high-bandwidth low-latency media (e.g., the use of optical fibers allows for a maximum distance of separation of 40 km between the RRH and its VBS) [3]. The communication functionalities of the VBSs are implemented on Virtual Machines (VMs) hosted over general-purpose computing platforms, which are housed in one or more racks of a small cloud datacenter. In a centralized VBS pool, since all the information from the BSs is resident in a common place, the BSs can exchange control data at Gbps. This can provide higher degree of freedom in order to make optimized and real-time decision so to improve the overall system performance.

Centralized management of computing resources, i.e., BS pooling, renders BS information global and, hence, enables cooperative communication techniques at the MAC and PHY layers that were previously not implementable due to strict inter-BS coordination requirements (in terms of throughput and latency). Although some recent works have studied the cooperative communication techniques that can benefit from C-RAN [5]–[7], research on enabling technologies for C-RAN itself is still at a nascent stage and, hence, there are only a few works in this area. The authors in [8] refer to C-RAN as Software Defined Radio (SDR) cloud and suggest hierarchical resource management where computing clusters are defined and assigned to different radio operators, cells, or services. In [9], the authors describe the virtual BS-pool structure and discuss key system challenges in implementing this concept.

They also propose a hybrid processing to match the workload of BS stack components. In [10], a partitioning and scheduling framework is proposed that is able to reduce the compute resources by 19%. In [11], the authors present a solution for small cells that reconfigures the fronthaul based on network feedback so to maximize the amount of traffic demand. In [12], a cooperative PHY/MAC solution is presented to address the inter-cell interference. In [13], the authors consider the C-RAN with finite-capacity backhaul links, and propose a hybrid compression strategy for downlink transmission to optimize the backhaul capacity utilization.

In summary, prior work on C-RANs focused on the overall system architecture, on the feasibility of virtual software BS stacks as well as on the performance gains. In contrast to existing works, we propose a novel cloud-based uplink solution supporting coordinated FFR that aims at improving the Signal-to-Interference-plus-Noise Ratio (SINR) and, hence, the overall system spectral efficiency, by fully exploiting the centralized advantages offered by C-RAN.

Our Contribution: In this paper, we leverage the advantages of FFR, CoMP, and CRAN and propose a novel uplink interference-cancellation solution to increase the system spectral efficiency while also decreasing both the intra- and inter-cluster interference. We first introduce the idea of "VBS-Cluster," in which we merge VBSs serving a cluster into a unit VBS-Cluster while the RRHs' antennae in each cluster act as a single coherent antenna array distributed over a cluster region. In the proposed solution, for each cell we define an Interference Region (IR); based on the IR of its neighboring cells, we then determine the Cell-Center Region (CCR). Since the cell-center MSs experience high level of SINR, we propose to apply CoMP processing only to cell-edge MSs, which leads to a decrease in the total complexity and latency. Moreover, in order to deal with inter-cluster interference, which is not addressed in traditional CoMP, we propose to exploit the cooperation of different VBSs for different cell-edge regions. We define the clusters of size 2 and 3 depending on the IR

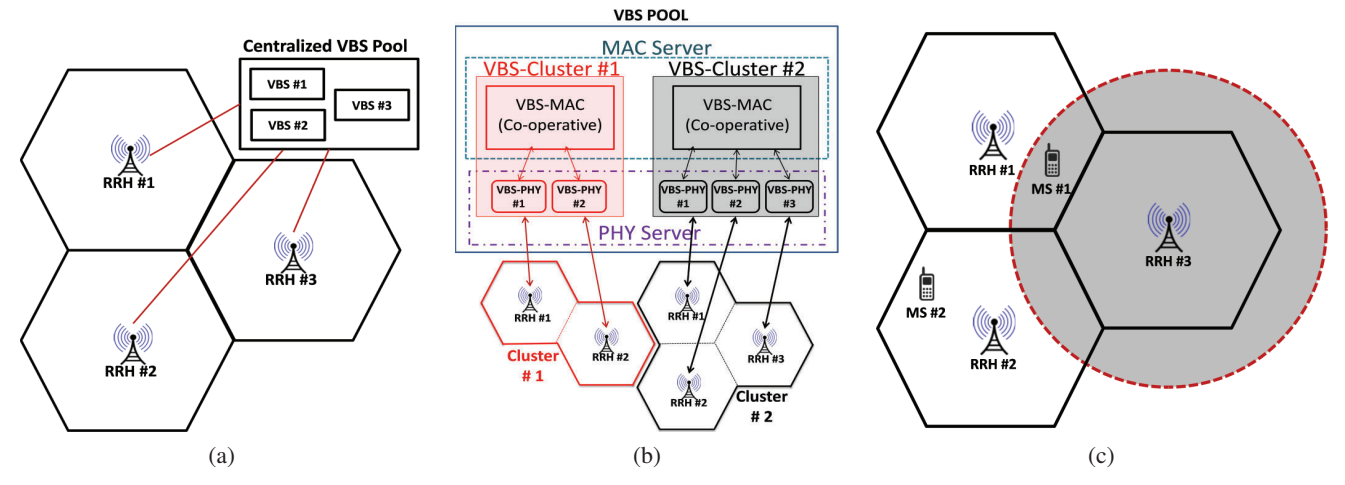


Fig. 2. (a) Cloud Radio Access Network (C-RAN) architecture, where the Base Stations (BSs) are physically unbundled into Virtual Base Stations (VBSs) and Remote Radio Heads (RRHs). VBSs are housed in centralized processing pools and can communicate with each other at Gbps speeds; (b) Virtual Base Station Cluster (VBS-Cluster); (c) The Interference Region (IR) associated with cell #3 (gray region) includes the cell itself as well as the neighboring Cell-Edge Regions (CERs)

intersection of neighboring cells; we partition the frequency band into 13 non-overlapping sub-bands, and allocate the frequency bands to the MSs based on the their position. In our solution, we also dynamically change the boundaries of sub-bands and optimize their widths in order to address the unanticipated fluctuations in the number of users and per-user capacity demands. This way, unlike the traditional OFDMA systems, the performance of the system in *all* the cell-edge regions relies on the cooperation of different VBSs, which avoids handover interruptions.

**Paper Outline:** In Sect. II, we present the system model and detail the issues with CoMP and FFR. In Sect. III, we introduce our solution, discuss its advantages, and explain how it decreases the average interference while increasing the system spectral efficiency with respect to (w.r.t.) current solutions. In Sect. IV, we validate our assumptions through simulations and show the benefits of our solution. Finally, in Sect. V, we draw the main conclusions and wrap up the paper by discussing future work.

#### II. SYSTEM MODEL

To understand better our proposed solution, we detail the issues with FFR and CoMP, and explain why these methods cannot overcome today's cellular network challenges.

FFR has been proposed as a solution to find a tradeoff between interference reduction and system spectral efficiency. In Strict FFR, the overall system frequency band is partitioned in such a way that, in a *cluster* of M cells, the MSs in the CCR are allocated a common sub-band of frequencies while the rest of the frequencies are equally partitioned into M sub-bands and assigned separately to Cell-Edge Regions (CERs) of the cluster. Figure 1(a) shows a cellular network using a Strict-FFR deployment where the cell-edge reuse factor is equal to 1/3. Since the cell-edge MSs use different frequency sub-bands than the cell-center MSs, the interference is reduced in both CCR and CER. With  $K_{tot}$  defining the total number

of available subcarriers, the number of subcarriers allocated to the cell-center MSs  $K_{center}$  and cell-edge MSs  $K_{edge}$  is given in [1] as,

$$K_{center} = \left\lceil K_{tot} \left( \frac{r_{center}}{r} \right)^2 \right\rceil, K_{edge} = \left\lfloor \left( K_{tot} - K_{center} \right) / M \right\rfloor,$$
 (1)

where  $r_{center}$  and r are the CCR and cell radii, respectively.

Although Strict FFR increases the SINR, only two subbands are allocated per cell in a cluster, which still leads to poor system spectral efficiency. In order to alleviate this problem, Soft FFR has been proposed. As shown in Fig. 1(b), in Soft FFR the frequency partitioning is the same as in its Strict counterpart, but the cell-center MSs are allowed to share sub-bands of CERs in the other cells. In Soft FFR, the allocation of subcarriers for cell-center MSs is the same as in Strict FFR, whereas the number of subcarriers allocated to the cell-edge MSs are given respectively as [1],

$$K_{edge} = \min(\lceil K_{tot}/M \rceil, K_{tot} - K_{center}),$$
 (2)

And yet, while Soft FFR increases the system spectral efficiency, it results in more interference to both cell-edge and cell-center MSs, leading to a high service outage probability. Moreover, in both Strict FFR and Soft FFR, the partition sizes are fixed and cannot adapt dynamically to the demand changes per region. This means that, as there is no coordination among the neighboring cells, changing the partition sizes in one cell may cause intensive interference in the other cells.

To solve the aforementioned problems and improve the system performance, we propose to use *both* CoMP and FFR under the C-RAN architecture. In CoMP, a set of neighboring cells is divided into clusters, and in each cluster the BSs coordinate with each other in order to improve the average SINR. Since in each cluster the BSs receive a combination of internal- and external-MS signals (Fig. 1(c)), the goal of CoMP is to cancel the intra-cluster interference (caused by internal

MSs from neighboring cells). We assume that there are M single-antenna BSs and N single-antenna MSs  $(N \leq M)$  in the cluster. Under these assumptions, the relationship between the received signals by internal BSs and the transmitted MS signals at different time instants can be expressed through the following linear noisy model (where, for clarity, the time variable t is omitted),

$$\mathbf{y}(k) = \sum_{j=1}^{N} s_j^{in}(k) \mathbf{h}_j^{in}(k) + \mathbf{n}(k) = \mathbf{H}_{in}(k) \mathbf{s}_{in}(k) + \mathbf{n}(k),$$

where  $\mathbf{s}_{in}(k) = [s_1^{in}(k), \dots, s_N^{in}(k)]^T$  is the  $N \times 1$  vector of internal MS signals over the  $k^{\text{th}}$  subcarrier,  $\mathbf{y}(k) = [y_1(k), \dots, y_M(k)]^T$  is the  $M \times 1$  vector of signals received by the internal BSs,  $\mathbf{H}_{in}(k)$  is the  $M \times N$  channel coefficient matrix between the MSs and BSs  $(\mathbf{h}_j^{in}(k))$  being its  $j^{\text{th}}$  column), and  $\mathbf{n}(k) = [n_1(k), \dots, n_M(k)]^T$  is the  $M \times 1$  background noise vector with independent components. It should be mentioned that in (3) we have included the intercluster interference as a part of the background noise, i.e.,

$$\mathbf{n}(k) = \mathbf{H}_{ex}(k)\mathbf{s}_{ex}(k) + \mathbf{w}(k), \tag{4}$$

where  $\mathbf{s}_{ex}(k) = [s_1^{ex}(k), \dots, s_L^{ex}(k)]^T$  is the  $L \times 1$  vector of the external-MS signals (causing inter-cluster interference),  $\mathbf{H}_{ex}(k)$  is the  $M \times L$  channel coefficients between the external MSs and internal BSs  $(h_{i,j}^{ex}(k))$  being its  $(i,j)^{\text{th}}$  component), and  $\mathbf{w}(k) = [w_1(k), \dots, w_M(k)]^T$  is the  $M \times 1$  vector of Additive White Gaussian Noise (AWGN).

A simple form of coordination is achieved by implementing a Zero-Forcing (ZF) receiver [6]. In a ZF receiver (for the uplink), since the CSI from all the BSs in a cluster is available, we can form the equalizer as  $\mathbf{G}_{ZF} = \left(\mathbf{H}_{in}^{\dagger}\mathbf{H}_{in}\right)^{-1}\mathbf{H}_{in}^{\dagger}$ , where the output of the ZF receiver is given by,

$$\hat{\mathbf{s}}_{in}(k) = \mathbf{G}_{ZF}(k)\mathbf{y}(k) = \mathbf{s}_{in}(k) + \mathbf{G}_{ZF}(k)\mathbf{n}(k), \tag{5}$$

where  $\hat{\mathbf{s}}_{in}(k) = [\hat{s}_1^{in}(k), \dots, \hat{s}_N^{in}(k)]^T$  is the  $N \times 1$  vector of estimated internal-MS signals, each of which is associated with a combination of the background noises at all the receivers. From (4) and (5), it is clear that CoMP is able to cancel the intra-cluster interference, but does not take any action to decrease the inter-cluster interference (which is incorporated in the background noise),

$$\hat{\mathbf{s}}_{in}(k) = \mathbf{s}_{in}(k) + \underbrace{\mathbf{G}_{ZF}(k)\mathbf{H}_{ex}(k)\mathbf{s}_{ex}(k)}_{\text{Inter-Cluster Interfernce}} + \underbrace{\mathbf{G}_{ZF}(k)\mathbf{w}(k)}_{\text{AWGN}}.$$

If we assume that the background noise at the  $l^{\rm th}$  receiver has a variance of  $\sigma_l^2$ , then the noise in the  $i^{\rm th}$  estimated MS signal has a variance of  $g_{i1}^2\sigma_1^2+\cdots+g_{iM}^2\sigma_M^2$ , where  $g_{ij}$  is the  $(i,j)^{\rm th}$  component of the equalizer matrix  $\mathbf{G}_{ZF}$ . It is clear from (6) that the interference generated by the external cluster-edge MSs dramatically decreases the SINR (due to the high absolute value of channel coefficient  $|h_{i,j}^{ex}(k)|$  between external cluster-edge MS and internal BSs) and has a severe destructive impact on the performance of the serving cluster.

#### III. PROPOSED SOLUTION

The intensity of inter-cluster interference is determined by the network topology, which depends on the MS distribution, the inter-site distance, and the distances between external MSs and internal BSs. In traditional CoMP, since only a group of BSs are connected to each other and can exchange data, the cluster boundaries are set and cannot be changed dynamically as needed. Consequently, we cannot do any high data rate exchange among the clusters (as required to enable cooperative interference cancelation), and messages between clusters need to travel over expensive backhaul links. Hence, CoMP only changes the boundaries of interference from cell to cluster. On the other hand, increasing the cluster size would lead to an increase in complexity to run the CoMP algorithms and also to an increase in the delay to exchange the CSI between MSs and BSs, which conflicts with the low-latency requirement of LTE systems. In addition, certain MSs (especially in CCR and close to BS) may only experience small interferers, which makes the CoMP with reasonable computational complexity largely ineffective.

Conversely, in C-RAN, all the VBSs of a large region are centralized in a common virtualized datacenter. This centralized characteristic along with real-time virtualization technology provides extra degree of freedom that is useful to mitigate both the intra-cluster interference as well as the inter-cluster interference. In addition, all the VBSs can communicate and exchange data with each other at Gbps speeds. Unlike in traditional cellular systems where each cell is only associated statically with a certain cluster, in C-RAN we are able to associate each cell with different clusters. We leverage these properties to form virtual clusters so to mitigate the intra-and inter-cluster interferences, to decrease the complexity of the system, and at the same time to boost the system spectral efficiency.

Virtual Base Station Cluster: Clustering the neighboring cells in a C-RAN architecture – together with enabling the coordination of the VBSs in the cluster – can improve the system performance by exploiting the extra degrees of freedom to make optimal decisions. Here, we introduce the idea of VBS-Cluster, wherein the VBSs associated with a certain cluster are merged together and the RRHs' antennae in each cluster act as a single coherent antenna array distributed over the cluster region. Figure 2(b) shows two exapmle VBS-Clusters, #1 (shaded in red, on the left) and #2 (dark shaded, on the right), where the sizes of the clusters are 2 and 3, respectively.

Coordinated FFR in the Cloud (Cloud-CFFR): In our Cloud-CFFR solution, we introduce a new clustering approach by exploiting the advantages of both FFR and CoMP as well as the capabilities of C-RAN to improve the overall system performance along different performance dimensions. Although the idea of Cloud-CFFR can be applied to any cell deployment, for simplicity we use regular hexagonal grid deployment (Fig. 2(c)). We define an Interference Region (IR) for each cell as a region in which if MSs from other cells moved in, they could produce an "intense" interference at the

BS serving the cell. Figure 2(c) shows three neighboring cells and the IR associated with cell #3 (in gray), which includes the cell itself as well as its neighboring Cell-Edge Regions (CERs). Here, both MS #1 and #2 are cell-edge MSs; in a system with a frequency reuse factor equal to 1, they may have destructive effects on the performance of their neighboring cells. Hence, their interference on the other cells needs to be canceled or mitigated to improve the overall SINR. Although MS #2 is a cell-edge MS, its interference at RRH #3 is low. This is because MS #2 is far from RRH #3 and, due to the path loss, the power of received signal (from MS #2) in the uplink at RRH #3 is low; hence, there is no need for VBS #2 and #3 to cooperate with each other in order to cancel the interference caused by MS #2 at RRH #3. Conversely, since MS #1 is in the IR of cell #3, there may be an intense interference from MS #1 to RRH #3; thus, coordination between VBS #1 and #3 is needed to cancel this interference.

In our solution, like in the traditional FFR, we partition the frequency band into 2 sub-bands, namely  $F_c$  and  $F_e$ , for cell-center and cell-edge regions, respectively. Then, as shown in Fig. 3(a), we further divide the cell-edge spectrum ( $F_e$ ) into 12 portions, each allocated to a certain cluster of VBSs to serve a certain region of cell edge. So, in each cell all the frequency band is used by the MSs and the frequency reuse factor of 1 is achieved.

Unlike in the traditional CoMP – in which the positions of MSs in the cell are not taken into account and all the BSs within a cluster cooperate with each other by exchanging CSI and MS signals – in our solution we divide the VBSs into virtual edge clusters based on the MS positions and minimize the number of coordinated VBSs so to bound the overall complexity and the delay associated with multiplesite reception/transmission as well as with CSI acquisition. In fact, we distinguish among the MSs based on their positions. We also leverage the C-RAN architecture and virtualization technology in such a way as to associate each VBS with different virtual edge clusters; this means that, for different areas of CER, each VBS coordinates with different VBSs in different virtual clusters, which increases the overall system performance. This way, only VBSs which have intensive interference from each other cooperate with each other to cancel the ICI. Figure 3(a) shows the intersections of IRs of 7 hexagonal neighboring cells. We define CCR as the area where there is no intersection between the IR of the serving cell and the IRs of its neighboring cells (central and pink in the figure). If we define the IR of the  $i^{th}$  cell as IR(i) then its CCR is defined as relative complement of union of the IRs of its neighbouring cells with respect to IR(i),

$$CCR(i) = IR(i) \setminus \bigcup_{j \in \mathcal{N}(i)} IR(j),$$
 (7)

where  $\mathcal{N}(i)$  is the set of neighbouring cells in the first tier of the  $i^{\mathrm{th}}$  cell.

Since the CCR of each cell is out of the IRs of its neighboring cells, the interference from this region to the neighboring RRHs is not intense; hence, applying CoMP in this region

would be highly inefficient due to the complexity, delay, and bandwidth usage to compute and exchange the CSI. Consequently, in our solution we do not apply computationally-expensive CoMP in CCR and the system performance in this region relies on simple single transmitter and receiver. To allocate the subcarriers to the CCR, we follow the strategy expressed in (1), as the number of allocated subcarriers is proportional to the CCR,

$$K_{CCR} = \left[ K_{tot} \left( \frac{A_{CCR}}{A_{cell}} \right) \right], \tag{8}$$

where  $K_{tot}$  is the total number of subcarriers,  $A_{CCR}$  is the area of CCR, and  $A_{cell}$  is the area of the cell site.

The system operation in cell-edge regions relies on the cooperation of different VBSs for different regions. Since we operate under the C-RAN architecture and all the VBSs are co-located in a common place (at the server, enclosure, or rack level in a datacenter), it is possible for each VBS to cooperate with all its neighboring VBSs and share the CSI as well as MS signals at Gbps. We define the CER of the  $i^{\rm th}$  cell as relative complement of CCR(i) with respect to IR(i),

$$CER(i) = IR(i) \setminus CCR(i),$$
 (9)

where, as shown in Fig. 3(a), CER(i) consists of different intersection regions each of which is the intersection of IR(i)with the IR of different neighbouring cells. We propose to divide the VBSs into clusters based on the intersections of their corresponding IRs in CER and apply CoMP within each cluster so to cancel the intra-cluster interference. This means that, in the cell edge and in each intersection region, the system performs under the cooperation of associated VBSs. For example, in the IR intersection of cells #1, #2, and #3, distinguished by bold lines on the right side of Fig. 3(a), the system performs under the cooperation of VBSs #1, #2, and #3. This is because MSs located in this (dark blue) region and served by each of these three VBSs #1, #2, and #3 induce an intense interference on the other two VBSs (non-serving VBSs). For instance, in Fig. 3(a), MS #1 (which is served by VBS #1) is inside the IR of cells #2 and #3 and may cause poor system performance to VBSs #2 and #3; however, since MS #1 is outside the IR of the other neighboring cells and is far from their corresponding RRHs, due to the path loss, it does not induce a large interference on their VBSs.

To generalize from this example, we can state that *in order* to improve the SINR of received signal by each RRH, we need to cancel the interference from those MSs located in its corresponding IR. This requires cooperation of each VBS with all its neighboring VBSs and in different clusters, which is only achievable in C-RAN architecture. Similarly, with reference to the aforementioned example for MS #1, in the IR intersection of cells #1 and #6, the gray area distinguished by bold line on the left side of Fig. 3(a), only VBSs #1 and #6 need to collaborate with each other. In this way, each VBS is simultaneously associated with 12 different clusters to serve different regions of cell edge. Similar to (8) where the allocated subcarriers to CCR is proportional to the area of

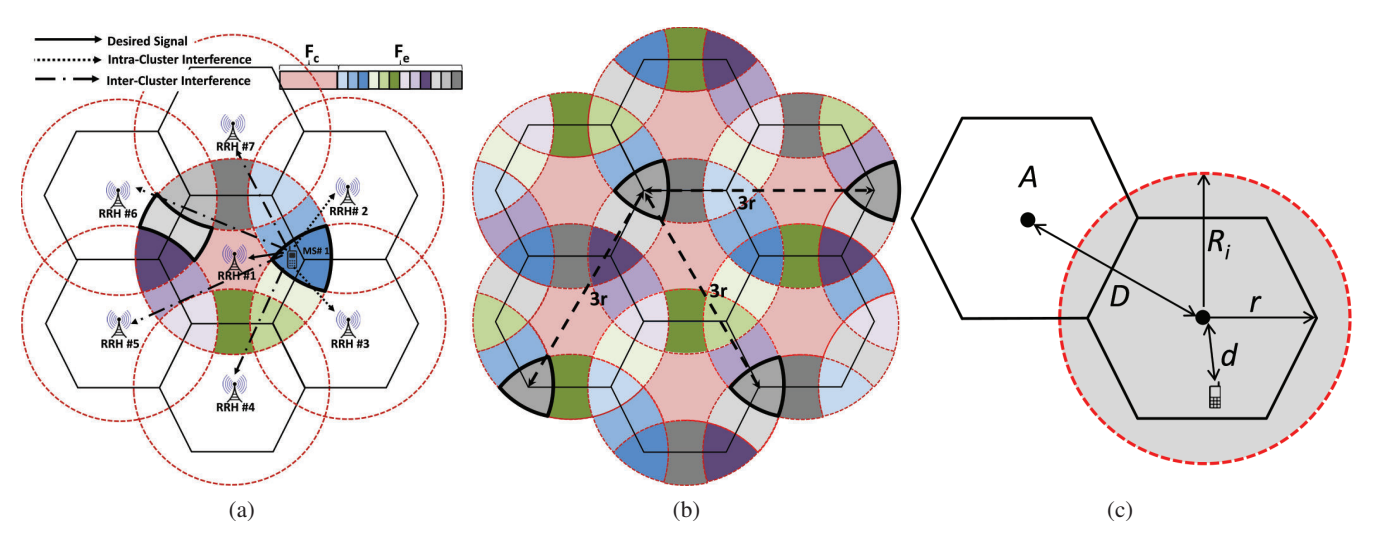


Fig. 3. (a) Intersections of serving cell's Interference Region (IR) with its neighboring cells' IRs; the MSs located in Cell-Center Region (CCR) have a low level of interference while the MSs located in Cell-Edge Region (CER) (e.g., MS #1) have an intensive interference on its neighbouring cells that needs to be cancelled; (b) The average distance between the MSs using the same subcarrier and located in the different clusters are 3 times of cell radius. The frequency reuse factor is equal to 1 and all the frequency band is used in each cell; (c) Equally sized hexagonal cell structures where r is the cell radius,  $D = \sqrt{3}r$  is the inter-site distance,  $R_i$  is the IR radius, and  $A = \frac{3\sqrt{3}}{2}r^2$  is the cell area.

CCR, the number of allocated subcarriers to each edge-cluster region is given by,

$$K_{CER}(p) = \left| K_{tot} \left( \frac{A_{CER}(p)}{M(p)A_{cell}} \right) \right|, \tag{10}$$

where  $K_{CER}(p)$  is the number of allocated subcarriers to the  $p^{\rm th}$  cluster (1 < p < 12),  $A_{CER}(p)$  is the area of the edge-cluster region, and M(p) is the cluster size.

As in our solution we only apply CoMP to CERs and the average cluster size is 2.5, the complexity and delay is reduced compared to traditional CoMP. Moreover, as depicted in Fig. 3(b), in our solution the MSs using the same frequency sub-bands and served by different clusters are so far from each other that each cluster induces a very low level of interference on the corresponding neighboring cluster. The average distance between the MSs using the same subcarrier and located in the different clusters are 3 times of cell radius, which is almost equal to the reuse distance of a cellular system with frequency-reuse factor of 1/3. Since in our solution CoMP cancels the intense intra-cluster interference and VBSs experience a small inter-cluster interference (due to the long average inter-cluster distance), we achieve a low level of interference on the received uplink signal. The SINR of received signals at ith RRH can be expressed as,

$$SINR_{Cloud-CFFR}^{i} = \frac{\beta_{i}P_{i}\left|h_{i,i}^{in}\right|^{2}}{\sigma^{2} + \sum_{j \in \mathcal{C}, j \neq i} P_{j}\left|h_{i,j}^{in}\right|^{2} + \sum_{l \in \mathcal{I}} P_{l}\left|h_{i,l}^{ex}\right|^{2}} + \frac{(1 - \beta_{i})P_{i}\left|\mathbf{g}_{i}^{zf}\mathbf{h}_{i}^{in}\right|^{2}}{\sigma^{2} + \sum_{l \in \mathcal{I}} P_{l}\left|\mathbf{g}_{i}^{zf}(\mathbf{k})\mathbf{h}_{l}^{ex}(k)\right|^{2}}$$

$$(11)$$

where  $P_i$  is the transmitted power of the MS located in the  $i^{\mathrm{th}}$  cell,  $\mathcal C$  is the set of cells in the serving cluster, and  $\mathcal I$  is the set of interfering external cells.  $h_{i,j}^{in}$  and  $h_{i,j}^{ex}$  are the  $(i,j)^{\mathrm{th}}$  components of  $\mathbf H_{in}$  and  $\mathbf H_{ex}$ , respectively.  $\mathbf g_i^{zf}$  is the  $i^{\mathrm{th}}$  row of the equalizer matrix  $\mathbf G_{ZF}$ ,  $\mathbf h_i^{in}$  and  $\mathbf h_i^{ex}$  are the  $i^{\mathrm{th}}$ 

column of  $\mathbf{H}_{in}$  and  $\mathbf{H}_{ex}$ , respectively, and  $\sigma^2$  is the power of the noise.  $\beta_i$  is the location indicator and is equal to 1 when the MS is located in the CCR of  $i^{\text{th}}$  cell and equal to 0 when the MS is located in the CER. We will analyse the SINR and compare it with different methods in Sect. IV.

Dynamic Frequency Sub-band: In Cloud-CFFR, we are also able to change dynamically the dedicated sub-band to each region. This leads to higher capacity and multiplexing gains without deploying additional antennae at the RRHs. In traditional FFR systems, due to the static spectrum resources, we are not able to handle unanticipated fluctuations in the number of users and per-user capacity demands. However, in some scenarios like natural or man-made disasters or due to the temporal/geographical fluctuations of MSs (the so-called tidal effect), the network may have more service demanding users in some regions. To address this problem, we propose to optimize the dedicated frequency sub-band to each cluster based on the number of active MSs in the clusters. Whenever in a certain cluster we have an overload and need to serve more MSs, the associated VBSs communicate with each other and dynamically change the sub-band boundaries so to increase the frequency sub-band for the overloaded region. If the associated VBSs have extra room in the other clusters and regions, they negotiate with each other and decrease the dedicated frequency sub-band of the other regions and increase the frequency subband of the overloaded region.

In the case of extra demand in the CCR of the  $j^{\rm th}$  cell, we allocate the unused subcarriers of edge-clusters to CCR. Let  $\mathcal{P}_{j}\left(p,k\right)$  be the subset of VBSs (including the  $j^{\rm th}$  VBS) serving the  $p^{\rm th}$  edge-cluster over the  $k^{\rm th}$  subcarrier  $(1 < k < K_{CER}(p))$  in CER of the  $j^{\rm th}$  cell and  $\mathcal{P}_{\bar{j}}\left(p,k\right) = \mathcal{P}_{j}\left(p,k\right) \setminus j$ . To avoid the excessive ICI caused by allocating the  $k^{\rm th}$  subcarrier of CER to CCR, VBSs in  $\mathcal{P}_{\bar{j}}\left(p,k\right)$  are not allowed to use the  $k^{\rm th}$  subcarrier. Conversely, in the case of extra

demand in some edge-cluster in the CER of the  $j^{\text{th}}$  cell, we allocate the unused subcarriers of CCR and the other edge-clusters to the overloaded edge-cluster. Let  $\mathcal{P}_j$  (p) be the subset of VBSs serving the  $p^{\text{th}}$  edge-cluster of  $j^{\text{th}}$  cell. Then, to avoid the excessive ICI caused by allocating the  $k^{\text{th}}$  subcarrier of the  $q^{\text{th}}$  edge-cluster to the overloaded edge-cluster (say the  $i^{\text{th}}$ ), the VBSs in  $\mathcal{P}_j$   $(q,k)\setminus\mathcal{P}_j$  (i) are not allowed to use the  $k^{\text{th}}$  subcarrier. However, in the case of allocating unused subcarriers of CCR to overloaded edge-clusters, there is no excessive ICI to the performance of  $\bar{\mathcal{P}}_j$  (q) and all the associated VBSs with the overloaded edge-cluster can use the subcarriers from associated CCRs.

**Handover Scheme:** In the Fourth Generation (4G) wireless networks, only Hard Hand-Over (HHO) (in which the connection between the serving BS and MS is terminated before the connection between the new BS and the MS is started) is defined to support MSs' mobility. As studied in [14], the service disruption time caused by HHO can be 250 ms or more, which is intolerable for some real-time services like Voice over IP (VoIP). On the other hand, with small cells, MSs perform handover more frequently leading to a decrease in the perceived Quality of Service (QoS). The degradation of QoS is a consequence of short interruption in communication during HHO due to redundant overhead generated for controlling and managing handovers. In our solution, cell-edge MSs are actively connected to 2 or 3 VBSs simultaneously so they do not have to terminate their connection with a serving VBS when they are moving from one cell to the neighboring cells. Hence, even with small cells and in a high-mobility scenario, MSs do not experience any service disruption as each MS operates under cooperation of multiple VBSs within a cluster.

### IV. PERFORMANCE EVALUATION

In this section, we analyze the behaviour of our proposed Cloud-CFFR solution in different regions and provide a range of simulations to evaluate its performance.

**Setting:** Table I lists the parameters used during our experiments. In the simulations, we use the equally-sized hexagonal cell structure with an inter-site distance D and cell radius r (Fig. 3(c)). MSs are uniformly distributed over the cell site and d is the distance between the MS and its serving RRH. To implement conventional CoMP, we consider a cluster with size 3. To compare Cloud-CFFR with Strict FFR and Soft FFR, we consider the structures showed in Figs. 1(a) and (b) with cell-edge reuse factor of 1/3 and CCR radius equal to 0.7r (which is the optimum CCR radius for M=3 [15]). Also, to have the same CCR for Cloud-CFFR, we consider  $R_i=1.3r$ , as illustrated in Fig. 3(c). In the simulations, we compare performance metrics among the traditional cellular network (without Inter-Cell Interference Coordination (ICIC)), CoMP, Strict FFR, Soft FFR, and Cloud-CFFR.

**Propagation Model and Discussion:** We concentrate on the effects of path loss and shadowing, and employ a commonly-used signal-propagation model as follows,

$$P_{rx} = K \cdot \left(\frac{d}{d_0}\right)^{-\lambda} \cdot \psi \cdot P_{tx},\tag{12}$$

where  $P_{rx}$ ,  $P_{tx}$ , d, and  $\lambda$  denote received and transmitted power, propagation distance, and path loss exponent, respectively; the parameter  $d_0$  indicates a reference distance where the received signal strength is known. The random variable  $\psi$  is used to model the slow fading caused by shadowing and follows a log-normal distribution such that the variable  $10\log_{10}\psi$  follows a zero mean Gaussian distribution. Finally, parameter K is a constant which corresponds to the path loss at distance  $d_0$  and depends on carrier frequency, antenna characteristics, and propagation environment. With this definition the channel between a MS and a RRH is  $h = \sqrt{K\psi} \left(\frac{d}{d_0}\right)^{-\lambda/2}$ . Hence, based on the system model and proposed solution presented in Sect. III, the SINR of received signals at  $i^{\rm th}$  RRH for different methods can be expressed as,

$$SINR_{StrictFFR}^{i} = \frac{\beta_{i}P_{i}|h_{i,i}^{in}|^{2}}{\sigma^{2} + \sum_{j \in \mathcal{C}, j \neq i} P_{j}|h_{i,j}^{in}|^{2} + \sum_{l \in \mathcal{I}} P_{l}|h_{i,l}^{ex}|^{2}} + \frac{(1 - \beta_{i})P_{i}|h_{i,i}^{in}|^{2}}{\sigma^{2} + \sum_{l \in \mathcal{I}} P_{l}|h_{i,i}^{ex}|^{2}},$$

$$SINR_{SoftFFR}^{i} = \frac{P_{i}|h_{i,i}^{in}|^{2}}{\sigma^{2} + \sum_{j \in \mathcal{C}, j \neq i} P_{j}|h_{i,j}^{in}|^{2} + \sum_{l \in \mathcal{I}} P_{l}|h_{i,l}^{ex}|^{2}},$$

$$SINR_{CoMP}^{i} = \frac{P_{i}|\mathbf{g}_{i}^{zf}\mathbf{h}_{i}^{in}|^{2}}{\sigma^{2} + \sum_{l \in \mathcal{I}} P_{l}|\mathbf{g}_{i}^{zf}(k)\mathbf{h}_{l}^{ex}(k)|^{2}},$$

$$(13)$$

According to (13) and (11), here, we explain how Cloud-CFFR increases the overall throughput with respect to the other methods.

TABLE I SIMULATION PARAMETERS.

| Parameters                             | Mode/Value                     |
|--|--------------------------------|
| Cellular Layout                        | Hexagonal grid, 19-cell sites  |
| Channel Model                          | Path Loss and Shadowing        |
| Cell Radius                            | 500 m                          |
| Channel Bandwidth $(\Delta B)$         | 10 MHz                         |
| Number of Occupied Subcarriers         | 600                            |
| Subcarrier Spacing                     | 15 kHz                         |
| CCR Radius for Soft FFR and Strict FFR | 0.7r                           |
| IR Radius                              | 1.3r                           |
| Distance-dependent Path Loss           | $38.88 + 32\log(d) \text{ dB}$ |
| Path Loss Exponent                     | 3.2                            |
| Carrier Frequency                      | 2.1 GHz                        |
| Number of Antennae $(N_{TX}, N_{RX})$  | (1,1)                          |
| MS Antenna                             | Omni-directional               |
| Channel State Information              | Ideal                          |
| Receiver Processing for CoMP           | Zero Forcing (ZF)              |
| Modulation Scheme                      | OFDMA                          |

Compared to the Soft FFR, since  $|h_{i,j}^{in}|$  in Cloud-CFFR is smaller (due to the higher path loss) than the one in Soft FFR we expect to have a better SINR for cell-center MS ( $\beta_i=1$ ). For cell-edge MS ( $\beta_i=0$ ), since there is no intra-cluster interference in Cloud-CFFR, we also expect to have a better performance than Soft FFR. Compared to the Strict FFR, the performance is the same for cell-center MS, but SINR for cell-edge MSs in Cloud-CFFR is less than the one in Strict FFR. This is because the number of interfering external cells in Strict FFR is less than Cloud-CFFR ( $|\mathcal{I}_{StrictFFR}| < |\mathcal{I}_{Cloud-FFR}|$ ). However, the number

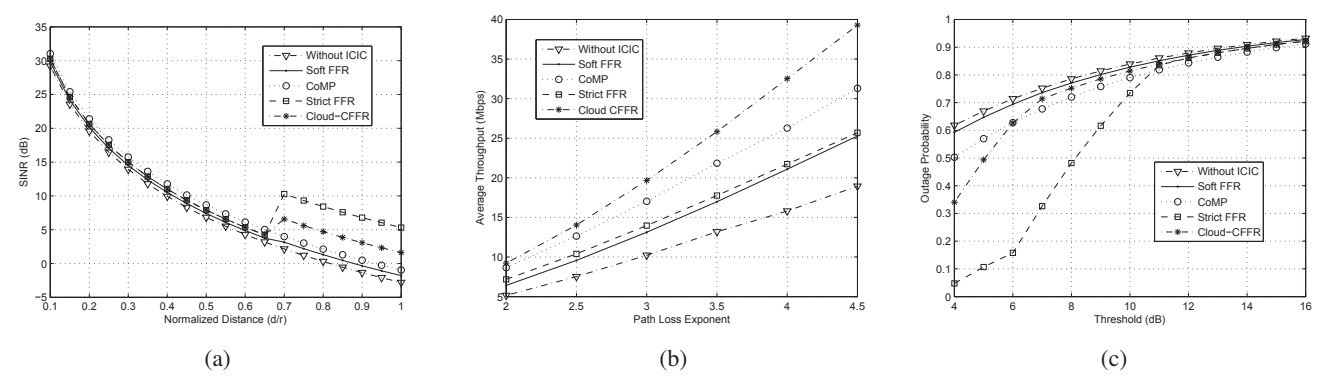


Fig. 4. (a) Signal-to-Interference-plus-Noise Ratio (SINR) for different Normalized Distances d/r; (b) Average Throughput per subcarrier for different Pass Loss Exponent  $\lambda$ ; (c) Outage probability for different thresholds in dB.

of available subcarriers per cell in Cloud-CFFR is 1.5 times more than the one in Strict FFR so that we expect to have more overall throughput with Cloud-CFFR (we will discuss about it through the simulations). Also, compared to CoMP, since the distance between the external MSs and internal RRHs is increased, the corresponding channel matrix in Cloud-CFFR has a smaller norm ( $\|H_{ex}^{Cloud-CFFR}\|_2^2 < \|H_{ex}^{CoMP}\|_2^2$ ) which results to have a better performance in terms of both SINR and throughput. Moreover, the complexity of Cloud-CFFR is much lower than CoMP. The complexity of CoMP algorithm depends on the numbers of cooperative RRHs (M), associated MSs (N), and subcarriers  $(k_c)$ . For instance, ZF receiver has a computational complexity of  $\mathcal{O}(k_c M^3 N^3)$  [16]. Since in CoMP the interference cancelation is applied to all the subcarriers ( $k_c = K_{tot}$ ), the system has an overall computational complexity of  $\mathcal{O}(K_{tot}M^3N^3)$ . However, in Cloud-CFFR the average cluster size is 2.5 ( $\overline{M} = \overline{N} = 2.5$ ) and ZF only is applied to the CER so that  $k_c = 0.5 K_{tot}$  which leads to have less computational complexity ( $\mathcal{O}_{\text{Cloud-CFFR}} = 0.22\mathcal{O}_{\text{CoMP}}$ ).

**Simulation Results:** To test and validate the aforementioned statements, in the first simulation, we compare the SINR in terms of Normalized Distance. As it is shown in Fig. 4(a), Cloud-CFFR outperforms both CoMP and Soft FFR in CER; however, Strict FFR has a greater SINR in CER. This is because Strict FFR uses a frequency reuse factor of 1/3 in CER and, according to (1) (for  $r_{center}=0.7r$ ), only use 66% of the frequency band. However, as we show next, the overall throughput of Strict FFR is less than that of Cloud-CFFR. Since the interference highly depends on path loss exponent, we also explore the variation of the average throughput of each subcarrier versus path loss exponent for different schemes. The throughput of each cell is given by,

$$R = \frac{k_0}{K_{tot}} \Delta B \log_2 \left( 1 + \text{SINR} \right), \tag{14}$$

where  $k_0$  and  $K_{tot}$  are the numbers of available subcarriers per cell and of total subcarriers, respectively, and  $\Delta B$  is the channel bandwidth. As shown in Fig. 4(b), for an urban area where the average path loss exponent is 3.5, Cloud-CFFR has an average throughput of 25.83 Mbps, whereas for Strict

FFR, Soft FFR, and CoMP the average throughput is 17.77, 16.98, and 21.84, respectively. As it is clear from Fig. 4(b), although Strict FFR has a better SINR in CER, its overall throughput is less than that of Cloud-CFFR. This is because Cloud-CFFR use all of the spectrum ( $k_0 = K_{tot}$ ), while Strict FFR can only use a portion of it ( $k_0 = 0.66K_{tot}$ ). We also examine the performance of our solution in terms of outage probability, which is the probability that a MS's instantaneous SINR falls bellow a certain threshold  $\theta$ , i.e.,  $\Pr(\text{outage}) = \Pr(\text{SINR} < \theta) = 1 - \Pr(\text{SINR} > \theta)$ . Figure 4(c) shows the variation of the outage probability in terms of different SINR thresholds.

In the other experiment we explore the performance of our solution for different SNR values. As it is shown in Fig. 5(a), Strict FFR does not have a good performance for low SNR values, while our proposed solution outperforms the other schemes for all the SNR values. For instance, for SNR= 20 dB, Cloud-CFFR has an ASSE of 2.32 bps/Hz/cell, while for regular CoMP, Soft FFR, and Strict FFR, the ASSE is equal to 1.97, 1.54, and 1.62, respectively. We also compare the Cumulative Distribution Function (CDF) concerning the SINR for different schemes; it is clear from Fig. 5(b) that for traditional network, Soft FFR, and CoMP, 20% of the MSs experience a SINR less than 0 dB. This means that the power of the received interference for 20% of MSs is greater than the power of received desired signal. However, in our solution all the MSs experience a SINR greater than 2.33 dB.

As discussed in Sect. III, to address the fluctuation in capacity demand, we propose to change dynamically the frequency sub-band boundaries. To examine this characteristic of Cloud-CFFR, we simulated the following simple scenario; let us assume that a set of cells have an equal number of MSs (in our simulation the number of MSs per cell varies from 50 to 200), each cell has 50 resource blocks to serve the MSs, and in each cell an active MSs needs 1 resource block to be served. We also assume that we have three types of cells: 1) cells where the probability of cell-center and cell-edge MSs to be active is 1/2 (i.e., density of active MSs in CER and CCR is equal), 2) cells where the probability of cell-center MSs to be active is 1/4 while the probability of cell-edge MSs to be

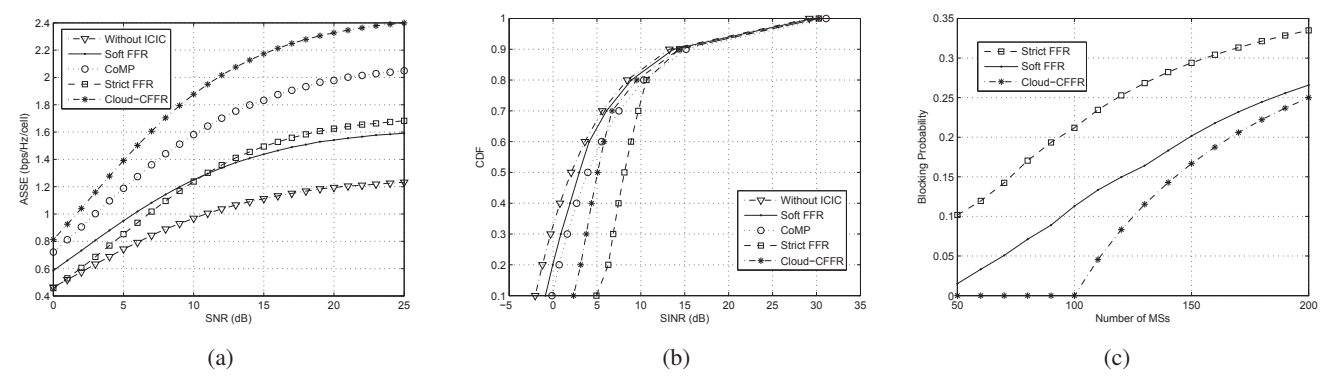


Fig. 5. (a) Average Spectral Efficiency as a function of Signal-to-Noise Ratio (SNR); (b) Cumulative Distribution Function (CDF) as a function of Signal-to-Interference-plus-Noise Ratio (SINR); (c) Comparison of Blocking Probability for different number of MSs.

active is 3/4 (i.e., the density of active MSs in CER is greater than CCR), and 3) cells where the the probability of cell-center MSs to be active is 3/4 while the probability of cell-edge MSs to be active is 1/4 (i.e., the density of active MSs in CCR is greater than CER). Each cell can be any one of the three aforementioned types with equal probability. Figure 5(c) compares the blocking probability when the number of users per cell increases; as it is shown, the blocking probability for Cloud-CFFR is less than the traditional network and we are able to serve more active MSs.

## V. CONCLUSION AND FUTURE WORK

In the context of Cloud Radio Access Network (C-RAN) we proposed and validated a novel solution, named Coordinated Fractional Frequency Reuse in the Cloud (Cloud-CFFR). Our innovative cellular-uplink solution mitigates the inter-cluster interference, the complexity, and delay while increasing the system spectral efficiency. We proposed to apply CoMP only to cell-edge MSs and exploit the cooperation of different VBSs for different cell-edge regions. Moreover, to address the unanticipated change in capacity demand, Cloud-CFFR dynamically changes the sub-band boundaries based on the number of active users in the clusters. Simulation results confirmed the validity of our analysis and show the benefits of this novel uplink solution. For instance, in the urban area Cloud-CFFR outperforms Strict FFR, Soft FFR, and CoMP in the average throughput by 45%, 52%, and 20%, respectively.

**Future Work:** To validate the proposed ideas on a real-time emulation, we are currently working on testbed implementation. The computer we use in the testbed is a Dell workstation with a 6-core Intel Xeon E5-1650 processor with 12 threads and 32GB of RAM. We also use Ettus B210 boards as Universal Software Radio Peripherals (USRPs) to establish communication between the BSs and the MSs. For each VBS, we run OpenAirInterface, an open-source LTE platform, on 64-bit Linux server and provision it with the required computing resources.

**Acknowledgment:** This work was supported in part by the National Science Foundation Grant No. CNS-1319945.

#### REFERENCES

- N. Saquib, E. Hossain, and D. I. Kim, "Fractional frequency reuse for interference management in Ite-advanced hetnets," *IEEE Wireless Communications*, vol. 20, no. 2, pp. 113–122, 2013.
- [2] D. Lee, H. Seo, B. Clerckx, E. Hardouin, D. Mazzarese, S. Nagata, and K. Sayana, "Coordinated multipoint transmission and reception in lte-advanced: deployment scenarios and operational challenges," *IEEE Communications Magazine*, vol. 50, no. 2, pp. 148–155, 2012.
- [3] D. Pompili, A. Hajisami, and H. Viswanathan, "Dynamic provisioning and allocation in Cloud Radio Access Networks (C-RANs)," Ad Hoc Networks, vol. 30, pp. 128–143, 2015.
- [4] C. M. R. Institute, "C-RAN: The Road Towards Green RAN," in C-RAN International Workshop, Oct. 2011.
- [5] A. Sang, X. Wang, M. Madihian, and R. D. Gitlin, "Coordinated load balancing, handoff/cell-site selection, and scheduling in multi-cell packet data systems," *Wireless Networks*, vol. 14, no. 1, pp. 103–120, 2008.
- [6] C. Wang, E. K. S. Au, R. D. Murch, W. H. Mow, R. S. Cheng, and V. Lau, "On the performance of the mimo zero-forcing receiver in the presence of channel estimation error," *IEEE Transactions on Wireless Communications*, vol. 6, no. 3, pp. 805–810, 2007.
- [7] S. Gollakota, S. Perli, and D. Katabi, "Interference alignment and cancellation," ACM SIGCOMM Computer Communication Review, vol. 39, no. 4, pp. 159–170, 2009.
- [8] V. Marojevic, I. Gomez, P. Gilabert, G. Montoro, and A. Gelonch, "Resource management implications and strategies for sdr clouds," *Analog Integrated Circuits and Signal Processing*, vol. 73, no. 2, pp. 473–482, 2012.
- [9] Z. Zhu, P. Gupta, Q. Wang, S. Kalyanaraman, Y. Lin, H. Franke, and S. Sarangi, "Virtual Base Station Pool: Towards a Wireless Network Cloud for Radio Access Networks," in ACM International Conference on Computing Frontiers (CF), May 2011.
- [10] S. Bhaumik, S. P. Chandrabose, M. K. Jataprolu, G. Kumar, A. Muralidhar, P. Polakos, V. Srinivasan, and T. Woo, "Cloudiq: a framework for processing base stations in a data center," in *International conference* on Mobile computing & networking. ACM, 2012, pp. 125–136.
- [11] K. Sundaresan, M. Y. Arslan, S. Singh, S. Rangarajan, and S. V. Krishnamurthy, "Fluidnet: a flexible cloud-based radio access network for small cells," in *International conference on Mobile computing & networking*. ACM, 2013, pp. 99–110.
- [12] A. Hajisami, H. Viswanathan, and D. Pompili, "Cocktail Party in the Cloud: Blind Source Separation for Co-operative Cellular Communication in Cloud RAN," Proc. of the IEEE Intl. Conf. on Mobile Ad hoc and Sensor Systems (MASS), pp. 37–45, 2014.
- [13] P. Patil and W. Yu, "Hybrid compression and message-sharing strategy for the downlink cloud radio-access network," *Proc. of the IEEE Information Theory and Applications Workshop (ITA)*, pp. 1–6, 2014.
- [14] W. Jiao, P. Jiang, and Y. Ma, "Fast handover scheme for real-time applications in mobile wimax," in *IEEE International Conference on Communications (ICC)*, 2007, pp. 6038–6042.
- [15] M. Assaad, "Optimal fractional frequency reuse (ffr) in multicellular ofdma system," *IEEE Vehicular Technology Conference*, pp. 1–5, 2008.
- [16] F. R. P. Cavalcanti, Resource Allocation and MIMO for 4G and Beyond. Springer, 2014.